Nucleation and growth of two-dimensional colloidal crystals

C.D. Dushkin [1], H. Yoshimura and K. Nagayama [2]

Protein Array Project, ERATO, JRDC, 5-9-4 Tokodai, Tsukuba, Ibaraki 300-26, Japan

We first grow two-dimensional crystals of nanometer latex particles from a thin film of water suspension placed on a flat solid substrate. The crystallization is performed by controlling the evaporation rate of water and the meniscus profile. The kinetic observations of the crystallization demonstrate two distinct processes: nucleation, preceded by thinning of the thin liquid film, and crystal growth. The crystal grows linearly in size, and its area increases as a quadratic function of time, due to the convective influx of particles from the suspension. A simple model of crystal growth interprets the kinetic data.

1. Introduction

Two-dimensional (2D) latex crystals [*1] have been prepared on solid substrates by drying up solvent from a suspension containing the particles [1–7]. These studies are concerned mainly with the final crystal, rather than with the crystal growth. Recently Denkov et al. [8] have created a new method of 2D crystallization of micron size particles on a glass plate by controlling the water evaporation from a latex suspension. They have illustrated that the crystallization is driven by directed motion of particles influxing to the crystalline area where the water evaporation is progressing. Until now, however, 2D crystals of nanometer latex particles have not been grown and the kinetics of their growth has not been studied. The purpose of our study is to produce 2D crystals of nanometer particles on a solid substrate by adopting the evaporation method. In addition, we aim to observe the whole view of the kinetics of the crystal growth by introducing a cell of millimeter size: The crystallization starts in the center of the cell and proceeds toward the periphery due to a concave meniscus profile extending over the cell. These attempts

may aid the understanding of the crystallization processes of protein macromolecules and many other globular particles.

2. Crystal growth process

Fig. 1 represents the experimental apparatus for the growth and observation of colloidal crystals. The crystallization cell is a circular hole of a diameter of 2 mm, pierced across a paraffin block (Nacalai Tesque, $20 \times 10 \times 5$ mm, melting point about 70°C). The block is sealed by a transparent substrate at the bottom by melting the paraffin surface. The substrate is either a glass plate (Matsunami, $18 \times 18 \times 0.17$ mm, washed with chromic acid) or a freshly cleaved mica plate. The cell area is 3.14 mm². We load the cell with 1 µl of water suspension of negatively charged latex particles (polystyrene latex, JSR) of 144 nm (± 2 nm) diameter and 0.001 volume fraction. The suspension spreads over the entire cell area in a layer with average thickness of about 300 µm. The meniscus profile is subconcave and the contact angle with the paraffin wall is 85° (± 5°). The upper side of the cell is kept open allowing the water to evaporate at constant temperature 20°C(± 2°C) and humidity 30%(± 3%). The crystallization is recorded by an optical microscope (Nikon, transmitted light) equipped with Super VHS video system (fig. 1a). Since crystals are slightly el-

---

[1] Permanent address: Laboratory of Thermodynamics and Physicochemical Hydrodynamics, Faculty of Chemistry, University of Sofia, 1126, Bulgaria.

[2] To whom correspondence should be addressed.

[*1] A two-dimensional (2D) crystal is referred to as monolayer to distinguish it from the multilayered 3D crystal.

       455
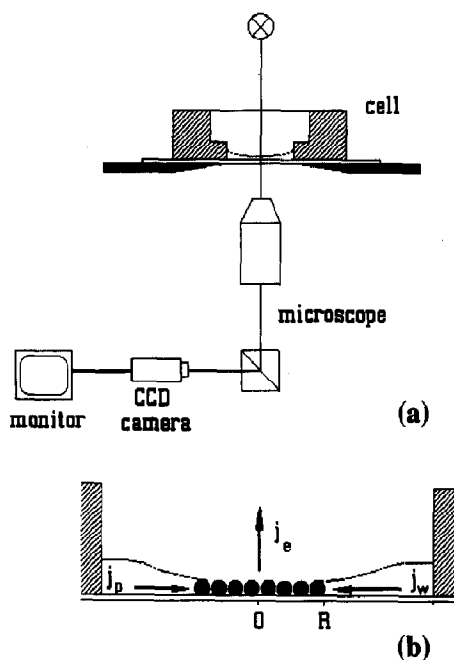
Fig. 1. Sketch of the experimental apparatus for producing and monitoring 2D crystals: total view (a), and crystallization cell with growing crystal (b).

liptic, two axes are measured from the video monitor using a calliper-gauge to calculate the crystal area with a maximum error of 10%. The structure of the final crystal is determined by a scanning and a transmission electron microscope (SEM 820 and TEM 1200 EX-II, JEOL) and by a scanning force microscope (SFM, Seiko).

The observation in situ reveals two processes of the crystallization: (i) *nucleation* and (ii) *crystal growth*. After loading the cell, the thickness of the suspension layer decreases gradually due to the evaporation of water. The concentration of the latex particles, which are seen to perform Brownian motion, increases. However, the layer always remains thinner in the center than in the cell periphery due to the subconcave meniscus. As a result, a thin liquid film forms at the central part of the cell after some period of evaporation (10–17 min). The film is plane parallel with radius of about 100 μm (fig. 2a). The initial film thickness (about 200 nm), estimated from the interference fringes, is higher than the particle diameter. The film drains within a few seconds until its upper surface presses the particles toward the glass,
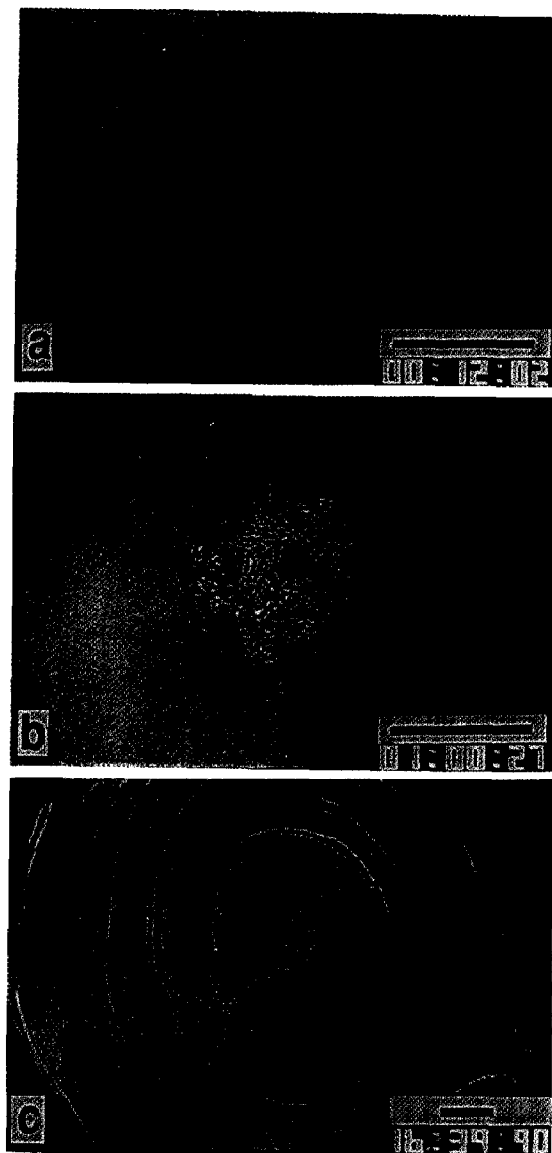

Fig. 2. Video image of the growing crystal: (a) thinning of thin liquid film preceding the nucleation (monochromatic light of wavelength 540 nm); (b) growth of circular monolayer crystal. The initial nucleus, which is of mesh-like structure with empty places, remains in the center; (c) the final crystal with area of 3.14 mm². The center is the monolayer from fig. 2b. Bars: 200 μm. Time in minutes (in this figure zero time coincides with the appearance of the thin film).

and they protrude from the film. The particles attract each other due to a sort of surface force acting in the lateral direction [9], resulting in the formation of a nucleus on the surface of the substrate. The nucleus is a circular monolayer which occupies the

thin film area and often contains small empty places (fig. 2b). Particles join the nucleus from the bulk suspension and a dense monolayer grows (fig. 1b). The meniscus area that encircles the nucleus shrinks as the crystal grows. In this process the water layer thickness near the crystal is almost equal to the particle diameter. At high magnification the video system has enough resolution to see the tracks of the particle flow. The particles are carried away and pressed against the crystal by water convective flow [8]. The water flowing into the crystal evaporates from its surface. Hence, the driving force of the particle influx is a water supply toward the crystal from the bulk. When the crystal approaches the cell periphery, the height of the meniscus near the crystal increases, resulting in multilayers formation. The growing speed of the crystal boundary in the lateral direction decreases, when multilayered crystals are formed, due to the nearly constant particle influx. At some moment the number of the layers starts to decrease due to the change of the meniscus profile and the growing rate comes back to the original one. As a result, the central monolayer is surrounded by alternating multilayer rings (fig. 2c). To produce crystals of only monolayer one should improve the meniscus profile to be uniform, for example by sucking or adding the liquid.

The monolayer and the multilayers have a hexagonal crystal lattice (fig. 3). In the transition zone between them a square lattice forms, gaining an intermediate thickness [10].

3. Kinetic model of convective crystallization

To explain the experimental data for the crystal area, plotted as a function of time in fig. 4a, we propose here a theoretical model for the crystallization process based on the convective mechanism [8]. For that purpose we consider the material balance of particles and water in the process. The number of the particles entering the crystal per unit time is

$$\frac{dN_p}{dt} = j_p A_h , \tag{1}$$

where A_h is the cross sectional area of the periphery of the crystal of thickness h, $dN_p = (1-\epsilon) \, d(hA)/V_p$, ϵ is the porosity of the crystal and $V_p = 1.56 \times 10^{-15}$
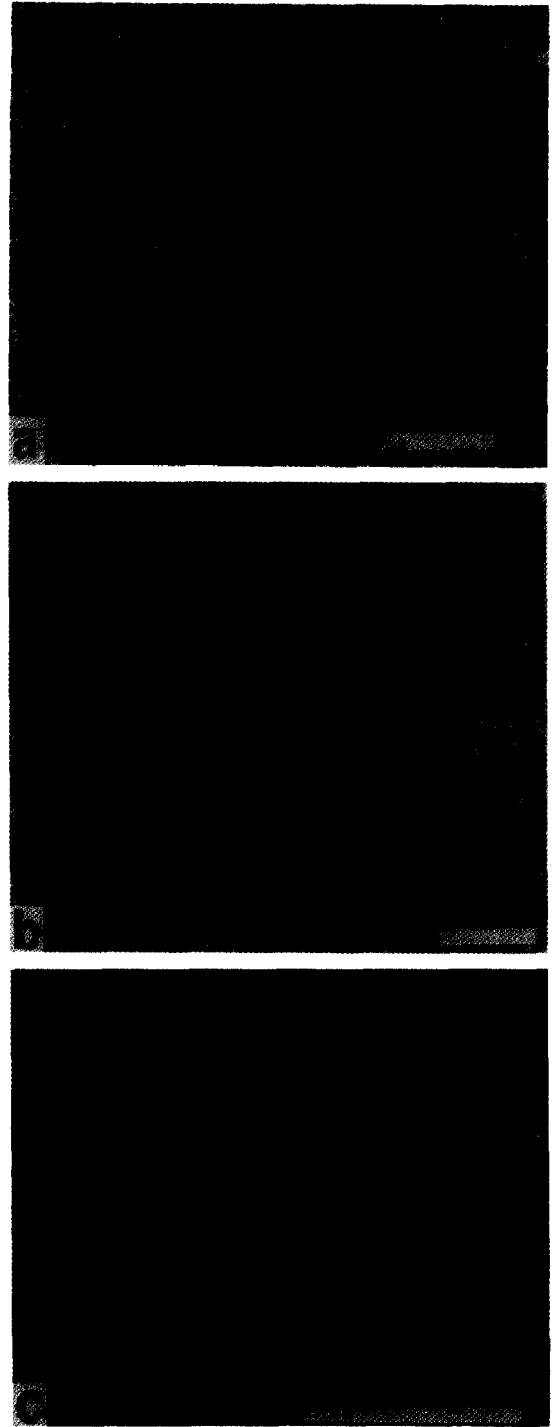
Fig. 3. Microscopic images of the monolayer crystal: (a) TEM, (b) SFM, and (c) SEM. Bars: 1 μm. The samples are coated by vacuum evaporation with carbon of about 5 nm thickness (for TEM and SEM) followed by gold coating (for SEM). For TEM the crystal is removed from the mica surface by floating the carbon film at the water surface. SFM images the crystal structure without coating.
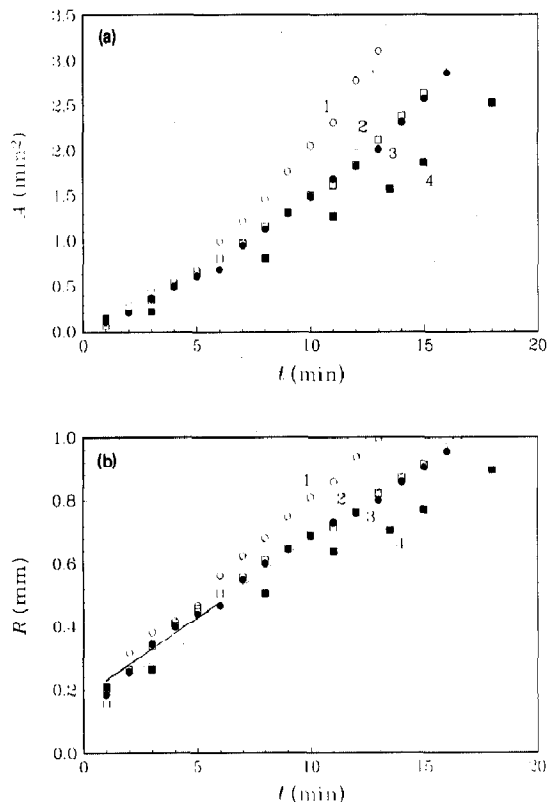
Fig. 4. Time dependence of the area (a) and of the mean radius (b) of three different crystals produced under similar conditions on glass and mica. The solid lines are drawn according to eq. (7) with the best fit for K from table 1.

cm^3 is the volume of a latex particle. The flux of particles is given by

$$j_p = j_w \beta \frac{V_w}{V_p} \frac{\varphi}{1-\varphi}, \tag{2}$$

where the water flux is $j_w = j_e A_e/A_h$, $\beta \leqslant 1$ is a factor accounting for the different hydrodynamic velocities of water and particles, $V_w = 3 \times 10^{-23}$ cm^3 is the volume of a water molecule, φ is the volume fraction of particles in the solution adjacent to the crystal boundary, j_e is the evaporation water flux and A_e is the area of evaporation from the crystal. From (1) and (2) we obtain an equation for the crystal area, $A(t)$

$$\frac{dA}{dt} = \frac{V_w j_e \beta}{1-\epsilon} \frac{\varphi}{1-\varphi} \frac{A_e}{h[1 + d(\ln h)/d(\ln A)]}. \tag{3}$$

To simplify eq. (3) we make the following as-

sumptions: (i) The crystal is, at all times, a circle with mean radius $R(t)$ ($A = \pi R^2$, $A_h = 2\pi R h$). (ii) The crystal thickness is nearly constant with time. Hence, the relative change of the thickness caused by the multilayering is much smaller than the relative change of the crystal area, i.e. $d(\ln h)/d(\ln A) \ll 1$. (iii) At the crystal boundary, the volume fraction of particles in the suspension, φ, and the hydrodynamic parameter, β, remain constant with time (stationary convection). (iv) The rate of water evaporation, j_e, is constant. To determine j_e we perform another experiment at constant area of evaporation A_e. Then the volume of water in the system decreases linearly with time

$$V(t) = V_0 - V_w j_e A_e t. \tag{4}$$

We obtain V by weighing the paraffin cell with pure water of initial volume of $V_0 = 1$ µl (here A_e is equal to the cell area). By fitting the experimental data for $V(t)$ using eq. (4) the water flux by evaporation is $j_e = 6.12 \times 10^{17}$ cm^{-2} s^{-1}. (v) The water evaporates only from the periphery of the crystal with a ring-shape area of constant width δ (the central part of the crystal is already dried). Hence, $A_e = 2\pi \delta R$ at $\delta \ll R$.

Solving (3) based on these assumptions, we obtain

$$A(t) = (\sqrt{A_0} + \sqrt{\pi} Kt)^2, \tag{5}$$

where $A_0 = A(0)$ corresponds to the nucleus area. Here

$$K = \frac{V_w j_e \beta \delta}{h(1-\epsilon)} \frac{\varphi}{1-\varphi} \tag{6}$$

is a constant. Eq. (5) predicts that the crystal area increases as the second power of time. This agrees qualitatively with the experimental data shown in fig. 4a. From (5) it follows that the crystal radius

$$R(t) = R_0 + Kt \tag{7}$$

depends linearly on time with R_0 being the nucleus radius. Hence, the quantity K defined by eq. (6) has the meaning of mean linear rate of crystallization. Although the local rate of crystallization, defined along a radial line, can vary with the number of layers, K is a constant because it characterizes the growth

of a crystal of circular shape and constant average thickness.

4. Numerical results and discussion

In fig. 4b we plot the mean crystal radius calculated from the experimental data in fig. 4a as $R = \sqrt{A/\pi}$. In table 1 are given the values of K determined by fitting the data using eq. (7) (the experiment numbers correspond to those from fig. 4a). The different slopes of the lines for crystals in fig. 4b, as well as the different periods of initial evaporation, are probably due to the differences in the experimental conditions: cell performance (because one paraffin cell is used for one experiment, a new cell is prepared for each crystallization), temperature (the evaporation flux j_e depends exponentially on the temperature) etc. There is no significant difference in the growth rate and structure of crystals produced on different substrates (glass or mica) at the same other conditions. The average rate of crystallization calculated from all the experiments in table 1 is 8.5×10^{-4} cm/s, indicating that approximately 60 particle rows join the crystal per second. The initial radius of the crystal R_0 in table 1 is determined by extrapolation of the kinetic data to zero time. This radius seems slightly larger than the initial radius of the nucleus from the video records. Actually, the physical radius of the nucleus cannot be known exactly because the nucleation is a random process resulting in nuclei of different area occupied by empty places. Also, the theoretical assumptions for deriving eq. (7) are questionable for the early stages of nucleation when the capillary force prevails.

To estimate an important parameter, the penetration depth δ in K, we assume that in average a monolayer crystal grows, i.e. $h = 144$ nm and $\epsilon = 0.395$ (for hexagonal packing). We accept also that water and particles move with close velocities which is reasonable for such small spheres ($\beta \approx 1$). Let us propose now that $\varphi \approx 0.1$. In fact, φ should be much larger than the initial fraction of latex in the suspension 0.001 but smaller than the fraction of latex in the crystal given by $1 - \epsilon = 0.605$. The calculated value of δ is about 40 μm which is always smaller than the crystal radius, R, confirming our assumption. Bearing in mind the definition of δ we conclude that the water penetrates most probably at a restricted distance inside the crystal. More accurately the value of δ could be found by considering the viscous flow of water along the pores inside the crystal.

In conclusion, we first grow 2D crystals of nanometer particles by convection driven crystallization and establish the kinetic law of the crystal growth. This type of crystallization is fast and the mechanism is different from that of three-dimensional (3D) crystallization of proteins in bulk solution [11]. Because the 3D crystallization is driven by diffusion of solute, it leads to a much lower rate of crystallization. Our method could be applied in the future to grow 2D crystals of proteins [12] and other fine particles.

Table 1
Crystal growth parameters

Experiment (substrate)	$K \times 10^3$ (cm/s)	R_0 (μm)	A_0 (mm²)
No. 1 (glass)	1.07	166	0.087
No. 2 (mica)	0.83	178	0.100
No. 3 (glass)	0.82	183	0.105
No. 4 (glass)	0.68	163	0.083

References

[1] T. Alfrey Jr., E.B. Bradford, J.W. Vanderhoff and J. Oster, J. Opt. Soc. Am. 44 (1954) 603.

[2] H.E. Kubitschek, Nature 192 (1961) 1148.

[3] W. Luck, M. Klier and H. Wesslau, Naturwissenschaften 14 (1963) 485.

[4] I.M. Krieger and F.M. O'Neill, J. Am. Chem. Soc. 90 (1968) 3114.

[5] J.A. Davidson and E.A. Collins, J. Colloid Interface Sci. 40 (1972) 437.

[6] H.W. Deckman and J.H. Dunsmuir, Appl. Phys. Letters 41 (1982) 377.

[7] S. Hayashi, Y. Kumamoto, T. Suzuki and T. Hirai, J. Colloid Interface Sci. 144 (1991) 538.

[8] N.D. Denkov, O.D. Velev, P.A. Kralchevsky, I.B. Ivanov, H. Yoshimura and K. Nagayama, Langmuir (1992), in press.

[9] P.A. Kralchevsky, V.N. Paunov, I.B. Ivanov and K. Nagayama, J. Colloid Interface Sci. 151 (1992) 79.

[10] P. Pieranski, L. Strzelecki and B. Pansu, Phys. Rev. Letters 50 (1983) 900.

[11] Z. Kam, H.B. Shore and G. Feher, J. Mol. Biol. 123 (1978) 539.

[12] H. Yoshimura, M. Matsumoto, S. Endo and K. Nagayama, Ultramicroscopy 32 (1990) 265.